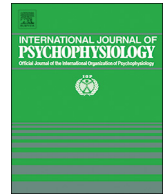




ELSEVIER

Contents lists available at ScienceDirect

International Journal of Psychophysiology

journal homepage: www.elsevier.com/locate/ijpsycho

Resting EEG effective connectivity at the sources in developmental dysphonetic dyslexia. Differences with non-specific reading delay

Jorge Bosch-Bayard^{a,*}, Katia Girini^b, Rolando José Biscay^c, Pedro Valdes-Sosa^{d,e}, Alan C. Evans^a, Giuseppe Augusto Chiarenza^{b,*}^a McGill Centre for Integrative Neuroscience (MCIN), Ludmer Centre for Neuroinformatics and Mental Health, Montreal Neurological Institute (MNI), McGill University, Montreal, Canada^b Centro Internazionale dei disturbi di apprendimento, attenzione e iperattività, (CIDAAI), Milano 20125, Italy^c Centro de Investigación en Matemáticas. A.C., Jalisco S/N, Col. Valenciana, Guanajuato 36023, Mexico^d The Clinical Hospital of Chengdu Brain Sciences Institute, University of Electronic Science and Technology of China UESTC, Chengdu, China^e Cuban Neuroscience Center, Cuba

ARTICLE INFO

Keywords:

Dysphonetic dyslexia
Non-specific reading delay
qEEG
Effective connectivity
Unleakage
Unmixing

ABSTRACT

Previous studies conducted on subjects with dysphonetic dyslexia (DD) reported inefficient timing integration of information from various brain areas. This dysregulation has been referred as neuronal dyschronia or timing deficiency. The present study examines the effective brain connectivity in Dysphonetic Dyslexic subjects (DD) compared to a group of subjects with non-specific reading delay (NSRD). The hypothesis is that the timing defect should be reflected also in the effective connectivity and the subjects with developmental dyslexia have an altered information flow different from the group of children with non-specific reading delay. The quantitative EEG at the sources of 184 children with DD was compared with that of 43 children with NSRD. The Isolated Effective Coherence (iCoh) was calculated among 17 brain regions data driven selected. To assess statistical differences in the EEG connectivity between the two groups, a Linear Mixed Effect (LME) model was applied. Two very important areas perform as hubs in the information flow: one is the left calcarine sulcus, which is more active in the DD group. The second is the left rolandic operculum, which is more active in the NSRD group. In the DD group, the calcarine sulcus is sending information to the right postcentral gyrus, the left paracentral gyrus, the right angular gyrus and the right supplementary motor area. This flow of information occurs in almost all frequency bands, including delta and theta band. Slow connections may indicate less efficient or even pathological information flow. We consider this as a neurophysiological evidence of Boder's model of dyslexia.

1. Introduction

Numerous clinical observations have reported that subjects with developmental dyslexia have difficulty in motor organization when they execute neuromotor tasks (Fog and Fog, 1963; Abercrombie et al., 1964; Connolly and Stratton, 1968) both simple (Denhoff et al., 1968; Lewis et al., 1970; Pyfer and Carlson, 1972; Bruininks and Bruininks, 1977) and complex (Owen et al., 1971; Klicpera et al., 1981). These difficulties in execution of motor tasks are associated with minor motor neurological signs as dysrhythmia, kinetic movements or mirror movements (Adams et al., 1974; Kennard, 1960; Stine et al., 1975; Wolff and Hurwitz, 1973). These motor impairments have been related with a disturbance in time organization in the performance of motor skills (Klicpera et al., 1981; Denckla, 1973). More recently, Nicolson

and Fawcett (2005) reported that dyslexic children have difficulties when required to undertake fast, fluent, over learned skills, or novel skills that involve the blending of two actions and their performance after extensive practice is slower and more error-prone. These multiple clinical and behavioral observations are further confirmed at the neurophysiological level. Llinás (1993) supports the hypothesis that at the base of dyslexia there might be a neuronal dyschronia that lead to inefficient integration of information from various brain areas.

Chiarenza et al. (1982) recording the movement related potentials, showed that subjects with dyslexia do not only suffer from a phonological or a gestalt deficit, but also from a praxic disorder in which praxic abilities, such as motor programming, sequential and sensory-motor integration and evaluation processes, are somehow defective (Chiarenza, 1990). A defect or an excess of absolute power in the

* Corresponding authors.

E-mail addresses: jorge.boschbayard@mcgill.ca (J. Bosch-Bayard), giuseppe.chiarenza@fastwebnet.it (G.A. Chiarenza).

various frequency bands in different brain areas have been frequently reported by many authors (Chabot et al., 2001; John et al., 1983; Duffy et al., 1980) using quantitative EEG (qEEG). Very recently Bosch-Bayard et al. (2018) comparing subjects with a dysphonetic dyslexia to subjects with a non-specific reading delay demonstrated that subjects with DD had significantly greater activity in delta and theta bands in the frontal, central and parietal areas bilaterally compared to the children with NSRD. All together these results clearly indicate that dyslexic children show a timing deficit or dyschronia in different brain regions which is evident both in the temporal and the frequency domain.

Recently, several researchers have investigated structural and functional connectivity in normal readers and in subjects with dyslexia.

Lou et al. (2019) using constrained spherical deconvolution tractography reported that the network connecting the left-occipital-temporal cortex and temporo-parietal cortex had decreased streamlines in dyslexic children suggesting a disconnection in a local subnetwork in the left hemisphere in dyslexia. Furthermore, Muller-Axt et al. (2017) using MRI and tractography reported that individuals with dyslexia have reduced structural connections in the direct pathway between the lateral geniculate nucleus and left middle temporal area V5/MT. Functional magnetic resonance imaging (fMRI) studies have highlighted three left-hemisphere areas which reveal an alteration in subjects with dyslexia (Shaywitz et al., 2002; Kronbichler et al., 2006). These regions are the parieto-temporal region, the inferior frontal gyrus, the occipito-temporal region, including the visual word-form area, responsible for rapid word recognition (Cohen et al., 2000; Cohen and Dehaene, 2004; Dehaene et al., 2005; Vinckier et al., 2007; Price and Devlin, 2011; Van der Mark et al., 2011). These areas and the homologous regions which are located in the right-hemisphere show either an over or an under activation during reading tasks in dyslexic subjects compared with non-impaired readers, in both children and adults (Finn et al., 2017; Horowitz-Kraus et al., 2016; Morken et al., 2017; Schurz et al., 2015; Shaywitz et al., 2002; Price and Mechelli, 2005; Shaywitz and Shaywitz, 2005; Richlan et al., 2011; Richlan, 2012).

Koyama et al. (2011) have also pointed out a stronger coupling among motor regions, as well as between language/speech regions. Besides, a greater connectivity has been found in subjects with dyslexia between the fusiform gyrus and the right anterior cingulate cortex (Horowitz-Kraus and Holland, 2015). In addition, Feng et al. (2017) showed an increased connectivity at the level of the cerebellum. Further hyper-connectivity has been described between cortical structures, such as lateral pre-frontal cortex, pre-motor cortex and subcortical structures, namely the thalamus (Fan et al., 2014). Similar results have been also obtained with qEEG. Hypo and hyper-connectivity have been observed in subjects with dyslexia in the occipito-temporal areas (Žarić et al., 2017), the frontal lobes (Horowitz-Kraus et al., 2016; Arns et al., 2007), and the central-parietal cortex (Stokić et al., 2011).

Using magnetoencephalography, Frye et al. (2012) demonstrated an increased gamma connectivity between the left temporo-parietal areas and other brain regions. Poorer phonological decoding was associated with increased influence of the right temporo-parietal areas on the inferior frontal areas and the ventral occipital-temporal areas in dyslexic children (Pugh et al., 2000).

These connectivity studies just referred to are based on measures of functional connectivity such as coherence which do not allow to infer effective connectivity.

The present study overcomes this limitation by examining the effective brain connectivity in dyslexic subjects compared to a group of subjects with non-specific reading delay. The hypothesis is that the timing defect or dyschronia should be reflected also in the effective connectivity and the subjects with developmental dyslexia have a different pattern of information flow compared to the group of children with non-specific reading delay. For this purpose, the Isolated Effective Coherence (iCoh) (Pascual-Marqui et al., 2014a, 2014b) between data-

driven selected regions is used as tool to quantify directed effective connections.

2. Material and method

2.1. Subjects

We used the same sample of subjects described in Bosch-Bayard et al. (2018). One-hundred-eighty-four subjects with dysphonetic dyslexia, 121 males (mean age 9.4; SD 1.9) and 63 females (mean age 8.8; SD 1.8) were compared with 43 children with non-specific reading delay, 26 males (mean age 9.9; SD 1.9) and 17 females (mean age 9.6; SD 2.4).

2.2. Clinical protocol

The following protocol was administered for the clinical assessment. By interviewing the parents, it was obtained information on a number of items: demographics, parents' qualification, medical and psychiatric history including the presence of language delay or specific language disorders, previous and concomitant medications and the eventual type of speech therapy performed during the first visit, after explaining the purpose and the procedures of the study the parents/caretaker, adolescents and children gave their informed consent. Then, physical and neurological examination, EEG, Amsterdam Neuropsychological Test (ANT) (De Sonneville, 2014), and a battery to test executive functions and attention, were carried out.

The dyslexia diagnosis was carried out according to the Diagnostic and Statistical Manual of Mental Disorders (*Diagnostic and Statistical Manual of Mental Disorders*, 2013) criteria with the administration of the following tests: (a) WISC III, (b) reading tests for primary school (Cornoldi and Colpo, 2011), and for secondary school (Cornoldi and Colpo, 2012) providing accuracy and speed scores in reading aloud age-normed texts, (c) single word and non-word reading, also providing speed and accuracy scores for each grade: the battery for the assessment of dyslexia and developmental dysortography (Sartori et al., 2007), and (d) the Direct test of Reading and Spelling (Chiarenza and Bindelli, 2001; Chiarenza, 2010). If the anamnesis indicates difficulties in mathematics, a battery for dyscalculia (Cornoldi et al., 2002; Cornoldi and Cazzola, 2003) or the battery for the assessment of developmental dyscalculia (Biancardi et al., 2004) were carried out. The presence of dysgraphia was assessed with Scala Sintetica per la Valutazione della Scrittura in Età Evolutiva (BHK) (Di Brina and Rossini, 2011) and Batteria per la Valutazione della Scrittura e della Competenza Ortografica (BVSCO) tests (Tressoldi et al., 2012).

In 48 subjects out of 184, dyslexia was associated with dysortography (26%), in 6 subjects with dysgraphia (3.3%), in 8 subjects with dyscalculia (4.3%), and in 14 subjects with dysortography, dysgraphia and dyscalculia (7.6%). Eight DD subjects had a previous diagnosis of Specific Language Disorder (SLD). Of these 8 subjects, five DD children received speech therapy lasting 12–48 months. Of the group of 43 subjects with NSRD, 11 subjects were dysortographic (26%), 2 subjects dysgraphia (4.7%), 3 subjects had dyscalculia (7%) and 4 subjects had dysortography, dysgraphia and dyscalculia (9.3%). One subject with NSRD had a previous diagnosis of specific language disorder (SLD). No therapy had been prescribed for this subject with NSRD.

The most frequent comorbidity in both groups was Attention Deficit and Hyperactivity Disorder (ADHD). In the DD group, 34 subjects (18.5% of total DD subjects) were affected by ADHD: 16 subjects (47.0%) had ADHD of inattentive subtype, 18 subjects (52.9%) had ADHD of combined subtype. In the group of subjects with NSRD, 12 subjects were affected by ADHD (28% of the total subjects with NSRD): 6 subjects had ADHD of inattentive type (50%), 5 subjects had ADHD combined subtype (41.7%) and 1 subject with ADHD not specified (8.3%). The 184 DD subjects had a mean Full-Scale Intelligent Quotient (FSIQ) of 101.4 (SD: 10.9), a mean Verbal Intelligent Quotient (VIQ) of

99.6 (SD: 11.7) and a mean Performance Intelligent Quotient (PIQ) of 103.4 (SD: 12.1). The 43 subjects with NSRD had a mean FSIQ of 105.5 (SD: 9.2), mean VIQ of 103.9 (SD: 12.1) and a mean PIQ of 106.6 (SD: 10.0).

All subjects had neurological examination within normal limits. None of the subjects had taken or were taking any type of drugs.

2.2.1. Exclusion criteria

Presence of documented psychiatric disorders in parents, a documented history of Bipolar disorders, history of psychosis or pervasive developmental disorder, seizure disorder, head injury with loss of consciousness or concussion, migraine, neurological/systemic medical disease (e.g., lupus, diabetes) or history of stroke or arterio-venous malformation or brain surgery were considered an exclusion criterion. Functional comorbidities such as visual or auditory processing problems were documented with IQ testing. The presence of ADHD or mild anxiety disorders were not exclusion criteria.

2.3. The direct test reading and spelling (DTRS)

The DTRS was used to identify the different subtype of dyslexia according to Boder's model (Boder, 1973) and the pattern of non-specific reading delay. The DTRS is a self-administered and self-paced task (Chiarenza and Bindelli, 2001; Chiarenza, 2010) that consists of a reading and spelling test. The reading test has 15 lists consisting of 20 words each, ordered by increasing difficulty according to numbers of syllables and orthographic difficulties. The first four are for the first grade of the primary school; the other 10, two for each grade, for the other five grades and the last one for the sixth grade. The subject decides spontaneously by pressing a button with the dominant hand to display on a screen the word to be read aloud. The words lists are presented in two ways: 'flash' and 'untimed' mode. In 'flash mode' the word appears for 250 ms, which determines the child's sight vocabulary (i.e., the words the child recognizes instantly as whole word configuration or gestalts). If he misreads the word or does not read it at all the child is asked to try again and, the word appears for 10 s 'untimed mode', which calls upon the child's ability to analyze unfamiliar words phonetically (i.e., his word analysis-synthesis skills). The highest-grade level at which the child's sight vocabulary includes at least 50% of the word list is considered his reading level (RL).

The spelling test is complementary to the reading test. It consists of dictating to the subject two lists of ten words each: a list of known words chosen from the 'sight vocabulary', and a list of unknown words, chosen from those unread or read with great difficulty during 'untimed mode' (i.e., not in sight vocabulary). Analysis of the spelling of 'known words' reveals the child's ability to 'revisualize' the words in his sight vocabulary, and analysis of the 'unknown words' list reveals his ability to spell words not in his sight vocabulary. Thus, the two spelling lists are designed to tap the central visual and auditory processes necessary for spelling, in the same way that the 'flash' and 'untimed mode' of the reading test tap the central visual and auditory processes necessary for reading.

At the end of the reading test the computer automatically provides the reading level ('RL'), the reading age ('RA'), and the reading quotient ('RQ'): the ratio between 'RA' and chronological age.

(CA) $RQ = (RA/CA) 100$. Finally, the identification of the dysphonetic reading-spelling pattern and that one of unspecific reading delay is based on the child's performance in three basic diagnostic indicators: % of words spelled correctly in the known list, % of words spelled correctly in the unknown list and the reading quotient. The dysphonetic pattern is present when the child has a percentage of words correctly spelled in the two lists < 70% and a reading quotient > 67; the non-specific reading delay pattern is present when the child has a percentage of words correctly spelled in the two lists > 70 and a reading quotient of < 90.

2.4. Neurophysiologic assessment and data analysis

2.4.1. EEG data acquisition

The EEG was recorded at 19 leads of the 1020 International Positioning System (S10–20), using Electro-caps referenced to linked earlobes (electrode impedances below 5000 Ohms, amplifiers with bandpass from 0.5 to 70 Hz). Twenty minutes of eyes closed resting EEG were recorded at sample rate 256 Hz with 12-bit resolution. A differential eye channel (diagonally placed above and below the eye orbit) was used for detection of eye movements. All EEG data were collected on the same digital system to achieve amplifier equivalence. All the patients were recorded in the morning and instructed to keep their eyes closed and stay awake. The technician was aware of the subject's state to avoid drowsiness. Additionally, patients were monitored with a closed-circuit television system.

2.4.2. EEG preprocessing

EEG experts visually edited the raw EEG data to select EEG epochs of stationary signals, free of transient events due to either biological (e.g., muscle movement, EMG) as well as non-biological (e.g., electrical noise in the room) artifacts. In this way, 30 artifact-free epochs of 2.56 s (256 time points at sampling rate 100 Hz) were selected for each subject.

The analysis of EEG signals to describe the background activity is based on the selection of quasi-stationary segments. This type of analysis does not include transient elements present in the EEG activity, which appear recurrently during an EEG recording. Taking epochs of 2.56 s is a quite common practice when analyzing EEG resting state to guarantee the stationarity of the signal. It has been demonstrated that the EEG background activity is composed of stationary segments with duration between 2 and 20 s (Jansen, 1979; Michael and Houchin, 1979; Niedermeyer et al., 2010 (Chapter 54); Praetorius et al., 1977). Since the signals are stationary, all epochs contain the same statistical properties and therefore, selecting 30 epochs of artifact free EEG is an adequate number for obtaining smooth statistical estimators of the subjects' brain signals, by averaging among epochs.

It should be emphasized that in our case, EEG segmentation is based only in human experts' visual selection, without the use of automatic procedures for cleaning the signals. Artifacts segments were not included in the analysis. Using the original raw EEG signals for the analysis ensures that the statistical properties are preserved, avoiding distortions produced by artifact removal software.

2.4.3. Unmixed estimation of the primary current at the sources

The EEG signal at each scalp location is the combined effect of primary (sources) at different places of the cortex, due to the volume conduction effect (Nunez and Srinivasan, 2009). This causes that calculating the brain connectivity between the EEG signals at the scalp does not show the real patterns of physiological connections in the brain. To overcome this, recent results suggest that brain connectivity analysis must be performed at the source level after applying some type of inverse method that infers the current sources from the scalp voltage.

However, such estimates of current sources attenuate, but do not completely eliminate the volume conduction issues (Biscay et al., 2018). There still remains some amount of mixing (blurring) of the signals at the estimated sources level (also known as the leakage problem) though it is more local than at the scalp voltage level, depending on the resolution matrix of the adopted inverse method (Biscay et al., 2018). They have a confounding effect in brain connectivity analysis at the estimated sources.

To overcome this drawback, we follow the methodology developed by Biscay et al. (2018). They provided a method, based on the analysis of the resolution matrix of the adopted inverse method, to solve the leakage at the sources (i.e., unmixing the signals) that works for any linear inverse method, such as the different versions of the Minimum Norm solution or the Loreta family.

They also demonstrated that there is a strong limitation for unmixing the signals at the EEG sources using linear methods which is that the highest number of EEG signals that can be unmixed at the sources is the number of electrodes minus 1. This is a general mathematical limitation which affects any kind of unmixing algorithm using inverse linear methods. This means that, for example, if the number of electrodes at the scalp is 128, it will be possible to obtain up to 127 unmixed ROIs. In our case, since our EEG recordings contain 19 electrodes, the maximum number of unmixed ROIs we can obtain is 18. However, to stay safe, avoiding the possibility of working in the boundaries of non-invertible matrices that can be created by 18 ROIs, we take only 17.

The method they proposed for unmixing the signals at the sources, while limited by the number of electrodes, can be applied both to the signal of individual voxels as well as to regions of interest (ROIs) as patches of the brain. The only requirement for these patches is that they must be disjoint, but they can cover or not the whole gray matter. The activity of the voxels inside each ROI is averaged by the method, so the solution that is obtained by such procedure is a constant piece-wise solution over all the ROIs. Therefore, the ROIs should be selected in a way that each one approximately represents a functional unit.

Thus, following Biscay et al. (2018), to obtain unmixed signals at the sources, the first step is to define the ROIs which signals will be unmixed. Since their number depends on the number of electrodes (19 in our case), we can define only up to 18 ROIs. To avoid working near the boundaries of singular matrices, instead of 18 ROIs, we only considered unmixing 17 ROIs. This guarantees more numerical stability of all procedures.

To select the 17 ROIs, different criteria may be used. One option is to select regions based in a previous neurophysiological knowledge of the areas we expect are more relevant to our problem. But this procedure may leave out areas which are in fact involved but have not been previously reported or that are out of our preconceptions. Another more realistic option is to select the ROIs by some data driven procedure, which extracts the ROIs more related to our interest from the data.

In our case, we choose the option of selecting the ROIs from a data driven procedure, which is described as follows:

- a) First, we estimate the current distribution over all the sources located in the gray matter. For this, we used the Montreal Neurological Institute (MNI) template (Evans et al., 1993, 1994) and a grid defined over its gray matter segmentation, which contains 3244 voxels covering the whole gray matter, i.e., it is a volumetric solution. We modeled the forward problem with a volumetric lead field using a 3 concentric spheres approach, according to (Riera and Fuentes, 1998), using the standard positions of the International 1020 electrodes system. To project back the EEG at the scalp to the sources we used the sLoreta (Pascual-Marqui, 2002) inverse method. Using sLoreta as inverse method is not critical for our purpose. Biscay et al. (2018) have demonstrated that the unmixing algorithm performs equally well for any linear inverse method. In this case, sLoreta was selected because it is easy to calculate and it also achieves the property of zero localization error, in one dipole simulations.
- b) The sLoreta algorithm was applied to each of the 30 epochs of artifact free EEG for each subject, described in Section 2.4.2. Estimates for the current at the 3244 voxels for each time point of each epoch and subject were obtained. This information is still in the time domain.
- c) To reduce spatial dimensionality, such source data were summarized by its average within regions, using the Automatic Anatomical Labeling (AAL) parcellation of the MNI template (Tzourio-Mazoyer et al., 2002), which divides the brain in 90 regions, excluding those belonging to the cerebellum. Although this atlas has been sometimes criticized for providing a rather coarse segmentation of some brain regions, especially the frontal regions, it is still one of the most used

- d) For each EEG epoch, a correlation matrix for the 90 regions was calculated. The correlations matrices of all epochs for each subject were averaged, producing one correlation matrix for each subject in each group. To make a more realistic estimate of the correlations among the regions, for each subject we eliminate 15% of the epochs with the higher and lower correlations, which may be considered as outliers.
- e) The correlation values were transformed to Z-Fisher scores, to obtain approximately Gaussian distribution.
- f) To find out which correlations were different between the two groups, t-student tests for all Z-Fisher scores were performed. They were corrected using the permutations technique to account for multi comparisons (Galan et al., 1994).
- g) Finally, we selected our 17 ROIs from the total number of ROIs which showed the higher significant differences between the groups.

Here we emphasize that the correlations analysis from d) to g) was only performed to select the potentially relevant ROIs but it was not used to assess the connectivity between the brain regions in the two groups. The reason for that is that correlations only captures not directed effective connectivity; they cannot differentiate from direct and indirect information flow and they cannot provide the direction of the information flow. After selecting the 17 ROIs, we have reduced the problem from epochs of 3244 sources to 17 sources in the time domain.

Finally, the algorithm described in Biscay et al. (2018) is then applied to the source time signals of the 17 ROIs to unmix them, eliminating the leakage effect that still remains after the inverse method. This prevents spurious dependencies in the connectivity analysis due to leakage, so providing clearer interpretation and neurophysiological relevance.

The unmixed signals are submitted to the connectivity analysis, as described below.

2.4.4. EEG based brain connectivity source analysis: assessing direct paths of intra-cortical causal information flow of oscillatory activity with the isolated effective coherence (iCoh)

To assess the causal connectivity patterns between the different brain regions in each subject, the “Isolated Effective Coherence” (iCoh) (Pascual-Marqui et al., 2014a, 2014b) is used. iCoh is a direct and directed measure of causal information flow in the frequency domain, developed under the concept of Akaike's Noise Contribution Ratio (NCR) (Akaike, 1968). Akaike's NCR is a spectral causality measurement that is even prior to Granger's causality, which was defined in the time domain (Granger, 1969). In fact, posterior causality measurements which have been understood as extensions of the Granger causality to the frequency domain (Baccala and Sameshima, 2001; Baccala et al., 2007; Kamiński and Blinowska, 1991; Saito and Harashima, 1981) are indeed nearer to Akaike's seminal concept than to Granger's (for a mathematical demonstration see Pascual-Marqui et al., 2014a, 2014b).

iCoh estimates the partial coherence among the nodes in a dynamic system under a multivariate autoregressive model, after setting to zero all possible variables associations, other than the particular directional association of interest. The partial coherence is a measure of association between two complex random variables after removing the effect of other measured variables. The difference between iCoh and NCR is that while NCR accounts for all connections direct and indirect without distinction among the nodes of the network, iCoh can separate direct from indirect connections keeping only the direct ones.

The iCoh index between any pair of variables (ROIs) X_i and X_j in a system, can be calculated in the two directions: from X_i towards X_j and from X_j towards X_i . The iCoh from X_i towards X_j is defined as the partial coherence between them (at each frequency) under a multivariate autoregressive model obtained from the original system, by setting all irrelevant associations (autoregressive coefficients) to zero, i.e., all

other associations except the one corresponding to the particular direct and directional influence of interest from X_i towards X_j . Unlike the correlation, iCoh is not symmetric and distinguishes between direct and indirect causal information flow, so capturing directed influences between the variables.

Pascual-Marqui et al. (2014a, 2014b) have shown in simulations and real data that iCoh is comparable to other types of causal information flow measurements like the popular Partial Directed Coherence (PDC) (Baccala and Sameshima, 2001), currently the most widely used method to measure effective brain connectivity. In general, iCoh exhibited a better performance than PDC to capture the real patterns of connectivity dominating a complex system.

iCoh has also been successfully used in resting-state EEG functional connectivity of different phases in migraine patients (Cao et al., 2016); to investigate causal transcallosal information transfer during auditory perception of simultaneous auditive stimulation of left and right ears (Steinmann et al., 2018); analysis of causal top-down signal transmission and hyper connectivity in auditory-visual synesthesia in EEG resting state (Brauchli et al., 2018); and to assess resting EEG effective connectivity differences of sleep onset transitions in humans before and after sleep deprivation (Fernandez Guerrero and Achermann, 2018). In all the previously cited papers, iCoh was used to successfully corroborate with novel findings, previous hypothesis about brain connectivity, which had not been yet proved with neurophysiological data. For more details and examples of the iCoh connectivity measure, see Pascual-Marqui et al. (2014a, 2014b). In what follows, we will simply call this method as causality analysis.

All calculations performed in this work were done by inhouse software developed in Matlab. However, the codes for sLoreta and iCoh have been repeatedly tested versus the results produced by the Loreta toolbox (Pascual-Marqui, 2002) and they produce the same results. The algorithm for unmixing the signals at the sources explained in Section 2.4.3 has not been included in the Loreta toolbox. All the code used here, together with an example of its use, can be found publicly available at https://figshare.com/articles/unmixing_test_m/6223778.

2.4.5. Statistical analysis

To assess statistical differences in the EEG connectivity between the two groups, a linear mixed effect (LME) model was applied. Specifically, for this analysis, we averaged the iCoh matrices of all epochs belonging to one subject, using the “median” function. After this, we kept 43 iCoh matrices for the NSRD group and 184 for the DD group. We used the LME model implemented in SURFSTAT (Worsley et al., 2009) to test group differences.

LME accounts for a mixed model of random and non-random effects. We specified “subject” as a random factor in the LME model to take into consideration repeated intrasubject data, and “group” as a non-random, fixed factor. Although the groups were unbalanced in number, they were well balanced by age. Nevertheless, we additionally considered the model including “age” as a non-random factor and the interactions between “age” and “group”. The analysis did not show significant contributions of these latter factors, so we finally considered the model which included only the non-random factor “group”, which has the additional advantage of dealing with a smaller number of parameters. The response variables in the model consist of the iCoh values between each pair of ROIs, at each frequency. In our case, we used a span of 32 frequency bins, from 1.5 to 45 Hz. Thus, the total number of response variables to be analyzed was 8704, which were analyzed individually through its corresponding LME model.

The permutations technique (Galan et al., 1994) was used to correct the thresholds of statistical significance for the high number of statistical comparisons.

To facilitate the report of the results we summarized them by frequency bands in the following way:

Delta (δ)	Theta (θ)	Alpha (α)	Beta 1 (β_1)	Beta 2 (β_2)	Gamma (γ)
1.5–3.5 Hz	4–7.5 Hz	8–12.5 Hz	13–20 Hz	20.5–35 Hz	35.5–45 Hz

Fig. 1 presents a summarized schematic diagram of the methodology steps.

3. Results

Thirty epochs of artifact free EEG were analyzed for 184 DD and 43 RR subjects according to the procedure described in Section 2.4.4.

To briefly illustrate the quality of the data that were analyzed, we provide additional plots as Supplementary Material. These plots show the mean EEG spectra and their standard deviation for each electrode at the scalp and each of the 17 ROIs selected for analysis for each group. Visual comparison between the two groups is also provided. These plots are not directly related to the purpose of this work, since we are not assessing group differences in spectral amplitudes or localizations but connectivity among different brain regions, which have already been reported in Bosch-Bayard et al. (2018). However, they are useful and easy to understand because this type of information is familiar in EEG research.

Table 1 shows the results of the significant t-student-tests of the brain regions correlations between subjects with DD and subjects with NSRD, after threshold correction by permutations. This result corresponds to the step f) of the procedure described in Section 2.4.4.

According to this table, many significant differences show a negative t-test, which indicates that the correlations are greater in the NSRD group. Additionally, many of the differences occur inter-hemispherical. Inside each hemisphere most of the differences appear in the right hemisphere.

3.1. Causality analysis

For the causality analysis, we reduced the number of ROIs to 17, according to Section 2.4.4. Based on the correlations results and considering that we were interested in describing differences between DD and NSRD groups, we selected those ROIs from Table 1 giving priority to those structures involved in reading disabilities.

In this case, we selected in the left hemisphere: calcarine sulcus, paracentral lobule, supramarginal gyrus, middle cingulum, and rolandic operculum. In the right hemisphere: postcentral area, lingual gyrus, inferior parietal gyrus, superior parietal gyrus, fusiform gyrus, superior frontal gyrus, paracentral lobule, rolandic operculum, middle cingulum, supramarginal gyrus, angular gyrus, temporal superior gyrus and supplementary motor area. Fig. 2 shows the distribution of the 17 ROIs in the gray matter.

We then reduced our data to those areas and performed the steps described in Sections 2.4.4 to 2.4.5. This procedure produced the causality results that are shown in Fig. 3, which is constructed from the statistical analysis of the iCoh measurements. To highlight the most significant changes between the two groups, we present the significant differences in connectivity at a threshold of 0.01, corrected by permutations in Table 2 and Fig. 3.

We additionally present a 3D view over the brain representation of the connectivity separated by bands in Fig. 4.

Table 2 shows significant differences of iCoh resulting from LME analysis of the causal Information flow among the 17 ROIs. The information flow goes from ROI 1 to ROI 2. Positive numbers mean greater connectivity in the DD group, while negative numbers mean greater connectivity in the NSRD group. The results are summarized by frequency bands as indicated in each column of the table.

In Fig. 2 the differences in connectivity are direct and directed. Therefore, it is possible to give a direction to the arrows. The arrows in red color between two structures indicate a significantly higher flow of

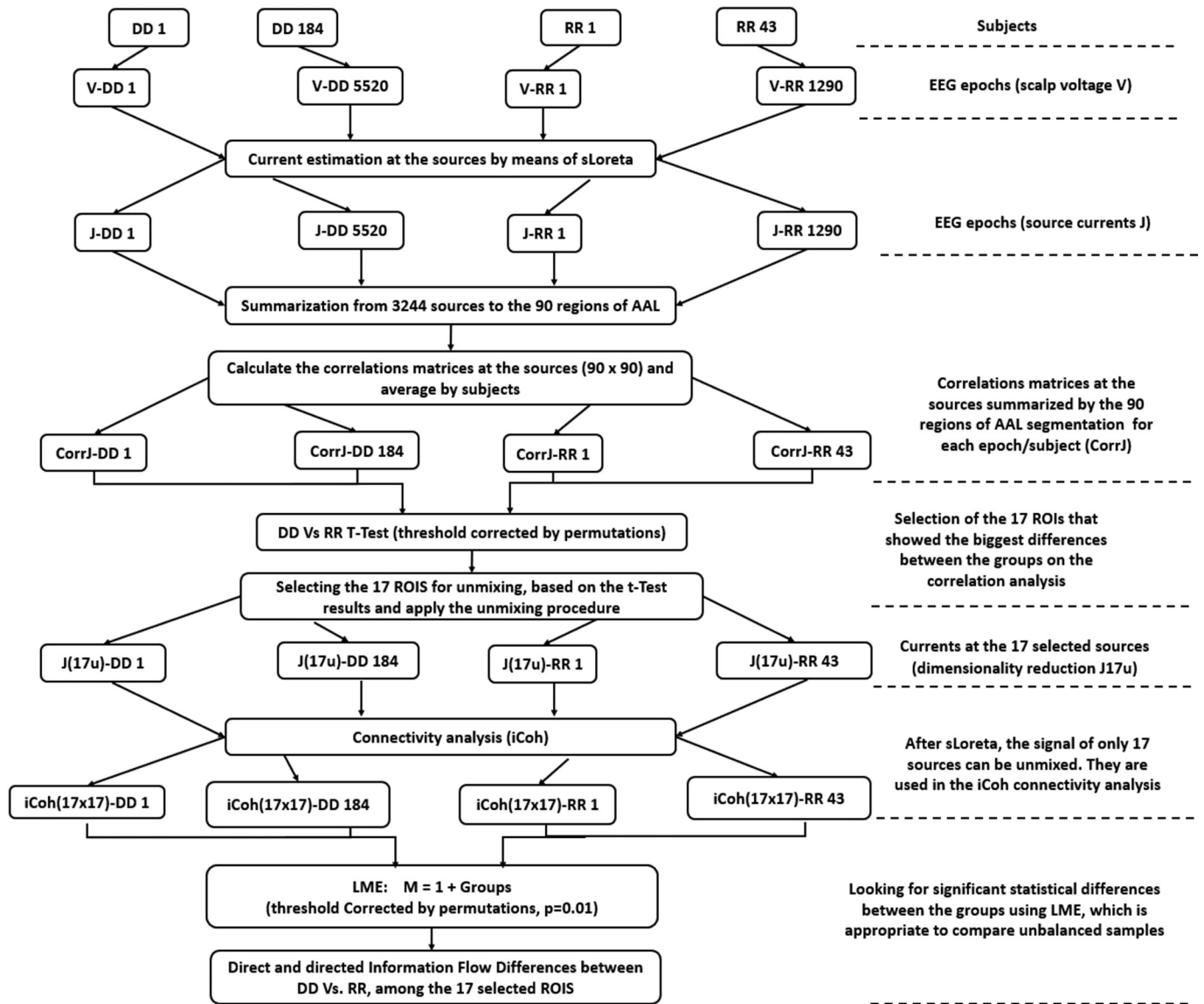


Fig. 1. A schematic diagram of the methodology presented in Section 2.4.

information in the DD group; the blue arrows indicate a significant higher flow of information between two structures in the NSRD. The Greek letters in the lines show the frequency bands in which the significant differences were found.

Two very important areas perform as hubs in the information flow: one is the left calcarine sulcus, which is more active in the DD group and the second is the left rolandic operculum, which is more active in the NSRD group.

In the DD group, the calcarine sulcus is sending information to the right postcentral gyrus, the left paracentral gyrus, the right angular gyrus and the right supplementary motor area. This flow of information occurs in almost all frequency bands, including delta and theta band. Slow connections may indicate less efficient or even pathological information flow.

On the contrary, there is another network that develops entirely within the right hemisphere almost exclusively in the beta1 band from the right fusiform gyrus, which shows two predominant pathways: a) to the right post-central gyrus and b) to the right inferior parietal gyrus which are both, in turn connected to the left rolandic operculum. The right inferior parietal gyrus is also connected with the right supra-marginal gyrus and the left rolandic operculum.

In the NSRD group the information flow occurs predominantly in

the high frequency bands beta1, beta2 and gamma. The core of this communication seems to be the left rolandic operculum which is more connected with the right inferior and superior parietal gyrus, the right angular gyrus, the right fusiform gyrus, the left calcarine sulcus and the left paracentral lobule which is, in turn, connected with the right angular gyrus.

At the threshold of 0.01, no significant differences appear between the right frontal, right supplementary motor area, right postcentral and right supramarginal gyrus.

4. Discussion

For the first-time using EEG brain connectivity, we can assess, in dysphonetic dyslexia and non-specific reading delay the causal flow of information among several important brain areas involved in the reading processes. This may contribute to shade light about the differences of information processing between these two groups with different degree of reading disabilities.

This analysis goes beyond than simply calculating correlations among sources, which is neither able to differentiate direct from indirect connections, nor to detect which structure is sending information and which structure is receiving.

Table 1
Significant differences in correlations between D D and NS RD groups, $\alpha=0.05$, corrected by permutations.

Brain Region 1	Brain Region 2	ttest	Brain Region 1	Brain Region 2	ttest
Precentral_R	Paracentral_Lobule_L	-3.68	H ippocampus_R	Cuneus_R	-2.64
Calcarine_R	Parietal_Inf_R	3.54	Cuneus_R	Occipital_Mid_R	-2.61
Postcentral_R	Cingulum_Mid_L	-3.50	Occipital_Mid_R	SupraMarginal_R	2.60
Cingulum_Mid_L	Paracentral_Lobule_L	-3.36	Hippocampus_L	Paracentral_Lobule_L	2.58
Supp_Motor_Area_R	Paracentral_Lobule_L	3.22	Frontal_Mid_R	Cingulum_Mid_L	-2.57
Precentral_R	Cingulum_Mid_L	-3.20	Parietal_Inf_R	Calcarine_L	2.55
SupraMarginal_R	Paracentral_Lobule_L	-3.14	Frontal_Mid_R	Paracentral_Lobule_L	-2.55
Frontal_Sup_R	Paracentral_Lobule_L	-3.06	Precentral_R	Frontal_Sup_R	-2.54
Frontal_Inf_Orb_L	Occipital_Inf_L	-2.98	Cingulum_Mid_L	Hippocampus_L	2.54
Temporal_Sup_R	Paracentral_Lobule_L	-2.97	Cuneus_R	Temporal_Pole_Sup_R	2.53
Frontal_Sup_Medial_L	Paracentral_Lobule_L	-2.95	Amygdala_R	Cuneus_R	2.53
Angular_R	Frontal_Mid_Orb_L	2.93	Temporal_Pole_Sup_R	Cingulum_Ant_L	-2.52
Fusiform_R	ParaHippocampal_L	2.92	Angular_R	Temporal_Mid_R	2.52
Olfactory_R	ParaHippocampal_L	2.82	Amygdala_R	Occipital_Sup_L	2.51
Postcentral_R	Paracentral_Lobule_L	-2.80	Frontal_Inf_Tri_R	Paracentral_Lobule_L	-2.51
Frontal_Sup_R	Cingulum_Mid_L	-2.80	Rolandic_Oper_R	Occipital_Inf_L	-2.51
Parietal_Sup_R	Parietal_Inf_R	-2.79	Occipital_Mid_R	Precuneus_R	-2.50
Frontal_Inf_Oper_L	Paracentral_Lobule_L	-2.76	Temporal_Pole_Sup_R	ParaHippocampal_L	-2.49
Frontal_Mid_R	Cuneus_R	2.75	Paracentral_Lobule_R	Paracentral_Lobule_L	2.49
Precentral_R	Insula_L	2.74	Olfactory_R	Paracentral_Lobule_L	2.49
Frontal_Sup_R	Cuneus_R	2.73	Parietal_Inf_R	Frontal_Sup_Orb_L	2.47
Angular_R	Frontal_Sup_Orb_L	2.72	Parietal_Sup_R	Angular_R	-2.47
Cingulum_Post_R	Cingulum_Ant_L	2.68	H ippocampus_L	ParaHippocampal_L	2.45
Frontal_Inf_Orb_L	Parietal_Inf_R	2.67	Precentral_R	Cingulum_Ant_L	-2.45

Additionally, it has been used for the first time an algorithm to unmix the signals at the sources, which eliminates spurious connections that still remain at the estimated sources after the application of an inverse solution method, such as sLoreta.

Our causality results show a more active connectivity in DD group from the left calcarine sulcus and the right lingual gyrus, which are part of the visual system, to other regions of the brain.

It is interesting to note that the significant differences associated to connections flowing from the left calcarine occur in almost all frequency bands, but primarily in the delta band to the right postcentral,

the right supplementary motor area and the left paracentral lobule. These are almost the only connections that occur in the delta band. We hypothesize that delta band may be associated to less efficient, dysfunctional or even pathological connections.

Visual inspection of EEG have revealed that the most common EEG abnormality is an increased generalized EEG slowing, associated with poor EEG rhythm, low-voltage background rhythms, high amplitude atypical alpha, abnormal focal paroxysmal activity, excess focal delta, persistent delta asymmetry, and excessive EEG response to hyperventilation (Hughes, 1978; Byring and Jarvilehto, 1985; Becker

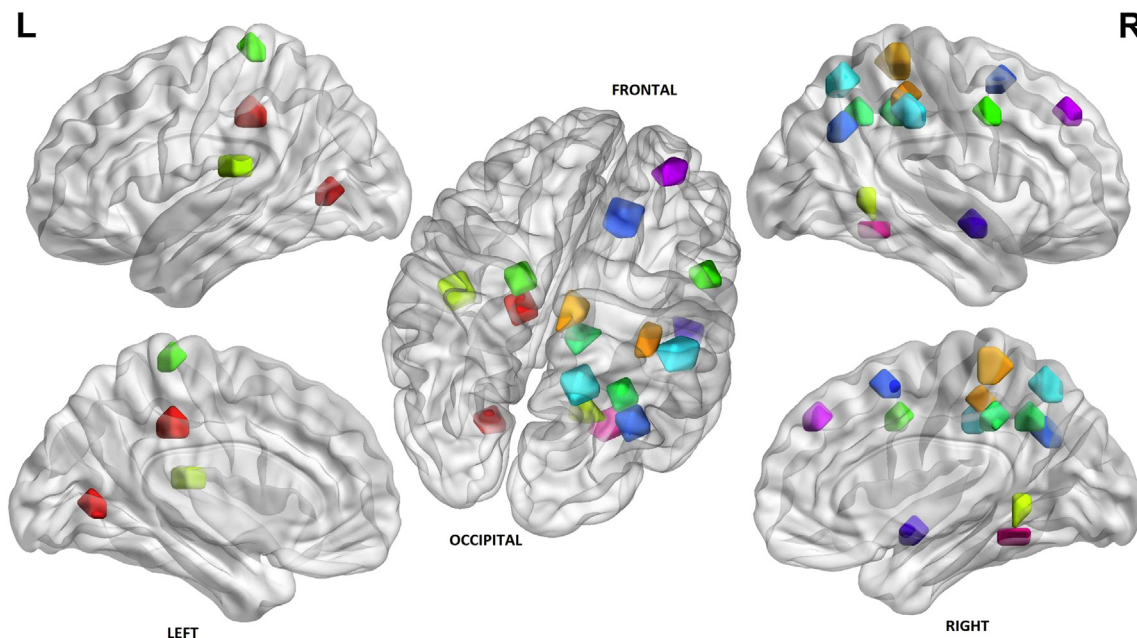


Fig. 2. Distribution of the 17 selected ROIs in the gray matter. The areas were selected by the data driven algorithm explained in Section 2.4.3. Only 4 ROIs were selected in the left hemisphere: paracentral lobule, supramarginal gyrus, middle cingulum, rolandic operculum and calcarine sulcus. Most of the ROIs were selected in the right hemisphere: postcentral area, inferior parietal gyrus, superior parietal gyrus, superior frontal gyrus, paracentral lobule, rolandic operculum, middle cingulum, supramarginal gyrus, angular gyrus, supplementary motor area, fusiform gyrus, temporal superior gyrus and lingual gyrus. Note that many of the ROIs are concentrated in the right parietal lobe. The different colors of the ROIs are only used to enhance visual inspection. The image was obtained using the BrainNet Viewer toolbox (Xia et al., 2013, <http://www.nitrc.org/projects/bnv/>).

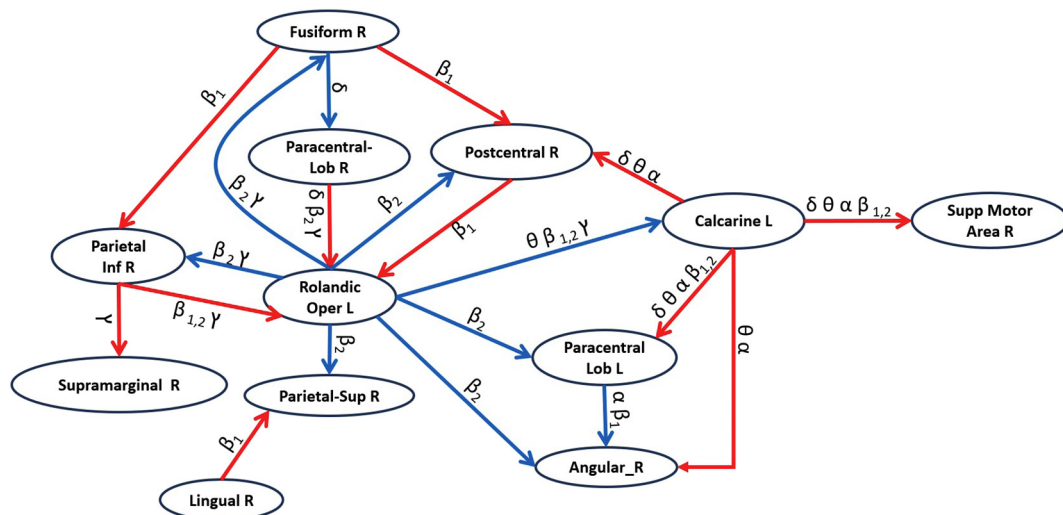


Fig. 3. iCoh differences between dysphonetic dyslexia and non-specific reading delay. Arrows in red color indicate that the iCoh information flow between two areas is higher in the DD group than in the NSRD group. Arrows in blue color indicate that the information flow between two areas is higher in NSRD group than in the DD group. In each line, there are annotated the frequency bands in which the differences were more significant.

et al., 1987; Byring et al., 1991). QEEG studies of eyes-closed resting EEG in dyslexic children showed a relative increase in low frequency (delta and theta) and a decrease in higher frequency activity (in particular alpha band) primarily in the left parieto-occipital area (John, 1981). QEEG abnormalities have also been shown to be directly related to academic performance carefully documented in both reading and writing. Harmony (1988) and Harmony et al. (1990) demonstrated that increased delta and/or theta power and decreased alpha power were associated with a poor educational evaluation; theta excess with alpha deficit was described as reflecting maturational lag, whereas delta excess indicated cerebral dysfunction (Harmony et al., 1990). More recently Arns et al. (2007) showed that dyslexics had increased slow activity (delta and theta) in the frontal and right temporal regions of the brain and increased beta1 specifically at F7. EEG coherence was increased in the frontal, central and temporal regions for all frequency

bands. Furthermore, a symmetric increase in coherence for the lower frequency bands (delta and theta) and a specific right-temporo-central increase in coherence for the higher frequency bands (alpha and beta) was also present.

Also, the right lingual gyrus in DD group sends more information to the right parietal superior area than NSRD group. Contrary to the above areas this flow of information happens only in the beta1 band. The right lingual gyrus plays a significant role in the reading process (Mechelli et al., 2000). It is an area of the medial occipito-temporal gyrus that is linked to the visual processes, color vision (Lueck et al., 1989; Corbetta et al., 1991; Zeki et al., 1991) and identification and recognition of words (Mechelli et al., 2000; Price et al., 1994; Bookheimer et al., 1995).

It may be interpreted as that the dysphonetic children tend to rely more on their visual abilities for reading words instead of their spelling

Table 2

Significant differences of iCoh, obtained from the LME among the 17 ROIs. The information flow goes from ROI 1 to ROI 2. Positive numbers mean greater connectivity in the DD group, while negative numbers mean greater connectivity in the NSRD group. The results are summarized by frequency bands as indicated in each column of the table.

ROI 1	ROI 2	Delta(δ)	Theta(θ)	Alpha(α)	Beta1(β_1)	Beta2(β_2)	Gamma (γ)	Total
		1.5-3.5 Hz	4-7.5 Hz	8-12.5 Hz	13-20 Hz	20.5-35 Hz	35.5-5 Hz	1.5-5 Hz
Calcarine_L	Postcentral_R	1.79	1.88	1.73				1.8
Calcarine_L	Paracentral_Lob_L	2.07	2.18	2.02	1.91	1.81		1.97
Calcarine_L	Angular_R		1.84	1.92				1.88
Calcarine_L	Supp_Motor_Area_R	2.44	2.46	2.46	2.06	1.73		2.2
Postcentral_R	Rolandic_Oper_L				1.75			1.75
Lingual_R	Parietal_Inf_R				1.85			1.85
Paracentral_Lob_L	Angular_R			-2.03	-2.06			-2.03
Parietal_Inf_R	Rolandic_Oper_L				1.72	1.72	1.82	1.8
Parietal_Inf_R	Supra_Marginal_R						1.82	1.82
Fusiform_R	Postcentral_R				1.71			1.71
Fusiform_R	Parietal_Inf_R				1.74			1.74
Fusiform_R	Paracentral_Lob_R	-1.98						-1.98
Paracentral_Lob_R	Rolandic_Oper_L	1.73				1.71	1.73	1.73
Rolandic_Oper_L	Calcarine_L		-2.04		-2.09	-2.43	-2.38	-2.33
Rolandic_Oper_L	Postcentral_R					-2.03		-2.03
Rolandic_Oper_L	Paracentral_Lob_L					-2.04		-2.04
Rolandic_Oper_L	Parietal_Inf_R					-2.07	-2.01	-2.06
Rolandic_Oper_L	Parietal_Sup_R					-2.04	-1.99	-2.02
Rolandic_Oper_L	Angular_R					-2		-2.0
Rolandic_Oper_L	Fusiform_R					-2.17	-1.97	-2.15
Rolandic_Oper_L	Cingulum_Mid_L					-2.25	-2.18	-2.22
Rolandic_Oper_L	Cingulum_Mid_L					-2.3	-2.2	-2.2

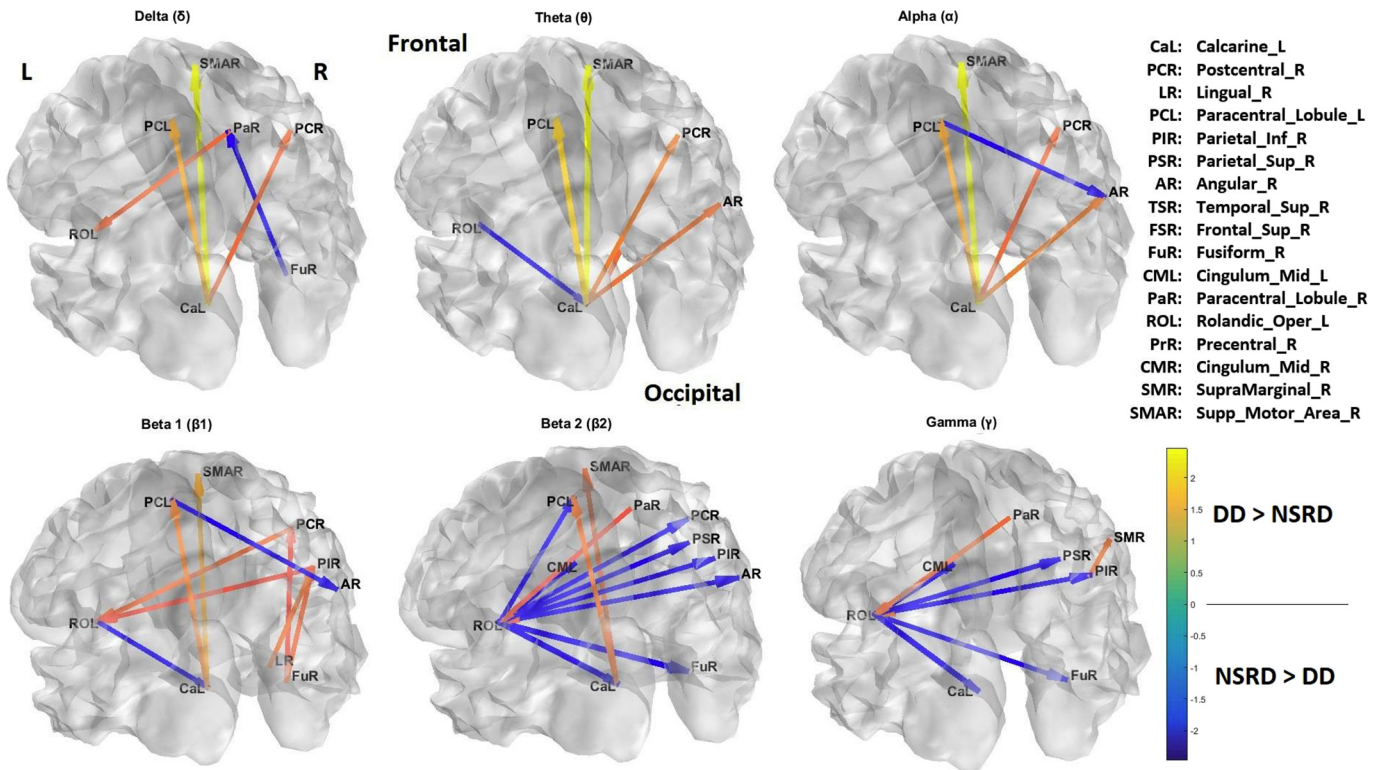


Fig. 4. Significant differences in functional connectivity between DD and NSRD groups summarized by bands, obtained by the iCoh procedure for $p = 0.01$, corrected by permutations. Negative values (blue colors) mean that the connectivity marked by the arrow is greater in the NSRD group. Positive values (red and yellow palette), on the contrary mean that the connectivity is greater in the DD group. Note that the arrows indicate the direction of the causal influence. Most of the blue arrows appear in the Beta 2 and Gamma band, which may indicate that the Left Rolandic Operculum behaves as a hub sending more information to a big number of structures in the NSRD group. The Left Calcarine sulcus is very active in the DD group sending information to parietal and temporal areas bilaterally in Delta, Theta and Alpha.

skills, according to Boder's assumption. This neurophysiological pattern is present even when a child is not involved in reading tasks but is in a quiet condition like recording an eyes closed resting EEG.

Boder's model of dyslexia proposes dyslexia as the result of an altered dynamic interplay between the auditory and visual areas involved in the reading process. Boder proposed that DD subjects tend to read words globally using the visual channel considered more efficient. They read the word as a gestalt rather than using analytical phonological processes. In fact, the most common misreadings are gestalt substitutions where the visual structure of the word is clearly recognizable, for the length of the word and the initial and final syllable, omitting often the central syllable.

Therefore, our results may be considered the first neurophysiological confirmation of the Boder's model using EEG signals at rest.

The only connection coming out from the left calcarine which does not involve delta band is towards the right angular gyrus which occurs in the theta and alpha band. The angular gyrus, together with the right supramarginal gyrus, forms a complex that receives somatosensory, visual and auditory inputs from the brain. They are believed to work together to link the words with their meaning, as a “neural mediator” of words and other meaningful symbols accessed through the visual system. It has been shown that the angular gyrus is active during numerous verbal tasks (Zatorre et al., 1996; Diamagnet et al., 1994a), less active in dyslexics during rhyme detection (Rumsey et al., 1992) and more active in dyslexics during orthographic identification (Flowers et al., 1991).

In this work we also found that the DD group sends increased significant connections from the right inferior parietal gyrus to the right supramarginal gyrus (Brodmann area 40), which is a portion of the parietal lobe that has been related with language perception and processing (Gazzaniga et al., 2009). In turn the right inferior parietal gyrus

receives more information from the right fusiform gyrus. This gyrus shows a greater activation in dyslexics during pronouncing or identifying phonologically regular non words (Kiyosawa et al., 1996; Diamagnet et al., 1994b).

In the NSRD group, the left rolandic operculum is much active than in the DD group. It is important to note that all connections coming out from the rolandic operculum occur in the beta and gamma bands. Improvements in the beta band at the posterior sites have been found in a group of dyslexic children, after receiving phonological training for six months (Penolazzi et al., 2010). Those children showed an increase of reading speed and a decrease in the number of errors during the reading process. Therefore, we hypothesize that connections in these frequency bands are most efficient, or more related to normal neurophysiological activity. Additionally, the left rolandic operculum had increased connectivity to structures in the right hemisphere (inferior and superior parietal gyrus, fusiform gyrus, angular and postcentral gyrus).

In a group of healthy children, Nakamichi et al. (2018) using near infrared spectroscopy (NIRS) found that the left rolandic operculum was involved in the phonological processing and articulation planning and execution of language. The children underwent two language tasks. In the task where they showed the best performance, they had more activations in the following areas: (i) the ventral sensory-motor cortex, including the rolandic operculum, precentral gyrus, and postcentral gyrus, (ii) the dorsal sensory-motor cortex, including the precentral and postcentral gyri, (iii) the opercular part of the inferior frontal gyrus, (iv) the temporal cortex, including the superior temporal gyrus, and (v) the inferior parietal lobe, including the supramarginal and angular gyri.

A further observation can be made about interhemispheric connectivity. The increased connectivity in the DD group from the left calcarine sulcus to the right postcentral gyrus and the right

supplementary motor area in the slow frequency bands may be in relation to the balance model described by Bakker (Bakker, 1992).

He described dyslexia as a sort of “failure” in the interhemispheric connection that would bring to two types of dyslexia. Premature reliance on left-hemispheric reading strategies may result in L-type dyslexia (L-type = linguistic type), which corresponds to Boder's dyseidetic dyslexia (Boder, 1973), characterized by a slow and syllabifying style of reading. On the contrary using right hemisphere reading strategies results in P-type dyslexia (P-type = perceptual type), which corresponds to Boder's dysphonetic dyslexia characterized by fast and inaccurate reading.

The difference between the two models lies in relation to a different denomination criterion. While the Boder's subtypes are named in accordance with the deficient function that is the cognitive domain which is functionally weak, the Bakker's subtypes are named according to the vicarious function that is the cognitive domain which is functionally preserved.

The increased connectivity from left rolandic operculum to right angular gyrus, superior and inferior parietal gyrus, right postcentral gyrus and right fusiform gyrus in the beta and gamma band, may explain why the NSRD group is more efficient than the DD in the reading process, since those structures play important roles during the execution of reading tasks. In this case, it is important to note that DD children have augmented flow of information from the left calcarine sulcus to the right angular gyrus in theta and alpha, while in the NSRD group there is a connection from the left paracentral lobule to the right angular gyrus in the alpha and beta bands. This fact, according to our hypothesis may indicate a more efficient connection to the angular gyrus in NSRD than in DD group. The participation of the angular gyrus in the reading process has been commented above.

The right and left paracentral lobules are highly involved in the information flow differences between DD and NSRD. The paracentral lobule is in the medial surface of the hemisphere, includes portions of the frontal and parietal lobes and it is the continuation of the precentral and postcentral gyri. The anterior portion of the paracentral lobule is often referred to as the supplementary motor area. This area receives from the left calcarine sulcus a significant higher flow of information in all frequency bands in comparison to NSRD group. Involvement of the motor areas in dyslexic subjects was described by Chiarenza et al. (1982) and Chiarenza (1990) recording the movement related potentials. From the analysis of these potentials Chiarenza (1990) concluded that dyslexic children besides being slow and not very accurate, present a deficit of programming movements, a deficit of visual and kinesthetic sensory integration and a reduced capacity to evaluate their performance and correct their errors.

Notably, there were no significant differences between the groups involving the right temporal superior and frontal superior gyri. Since these are structures related to the reading process, to our understanding it means that there are no differences between the two groups in the way the process the information in those structures, which is also another relevant finding.

These results are consistent with our previous study conducted on the same subjects. We combined the reading and writing performance of the DTRS with the QEEG and subjected them to the Stability based Biomarkers identification methodology in order to identify which variables were able to differentiate the DD subjects from the NSRDs. The variables associated to phonological processes of the reading test were not selected in the classification equation. On the contrary dysphonetic and dyseidetic errors during the writing were selected in the classification equation (Bosch-Bayard et al., 2018). These subjects showed difficulties when they had to convert the visual string of a word in a sequence of motor acts.

5. Limitations and future work

5.1. Validity of estimating primary current at the sources from a 19-electrodes EEG recording

The issue of estimating the distribution of the primary currents at the sources using a low-density electrodes array EEG has been widely discussed in the past. Comprehensive discussions of this issue have been published elsewhere (Grech et al., 2008; Michel and Brunet, 2019; Ryyänen et al., 2004; Song et al., 2015). In general terms, the two main factors affected by the number of electrodes are the localization error and the point-spread function (PSF) of the estimation at the sources. However, these two parameters do not depend only on the density of the electrodes array but also on the level of noise in the data, the deepness of the sources and the scalp thickness. It has been demonstrated that the PSF decreases with a higher number of electrodes, while a small number of electrodes produce very blurred solutions. However, to get advantage of high-density electrodes array it is necessary to have good quality data. As the noise in the data increases, the advantage of having higher electrode arrays decreases (Ryyänen et al., 2004). In terms of localization error, it also depends on the inverse solution method: while sLoreta produces very blurred solutions, with one of the poorest PSF, the use of 19 electrode channels array does not affect its zero-localization error property.

Additionally, a recent review (Asadzadeh et al., 2019) of EEG inverse methods has found that sLoreta and Loreta are the most popular inverse methods used in the literature. At this point we should emphasize that after applying our unmixing algorithm, the localization error becomes zero for all unmixed sources, independently of the linear inverse method used (Biscay et al., 2018).

Another important point to mention is that the inverse solutions are not only affected by the number of electrodes but also for their distribution all over the scalp. Regarding the 10–20 system, it does not include electrodes over the inferior part of the head which can lead to mis-localization of activities originating from the mesial temporal lobe (Michel and Brunet, 2019).

One should recall that not always a higher number of electrodes means better performance. With very dense electrode arrays, the technical difficulties to get a clean recording increase, as well as the possibility of obtaining lower quality recordings and more artifacts. Also, the risk of having saline bridges and spurious hyper correlations increases. Many studies conclude that electrode arrays between 32 and 64 are more recommended than 128 and 256 electrodes systems.

A search in Google Scholar for “sLoreta” and “10-20 EEG system” produced > 100 results (Babiloni et al., 2004; Eugene et al., 2015; Imperatori et al., 2014). This is an evidence that the number of electrodes affect but is not the most critical factor. (Michel and Brunet, 2019) say that “Even with < 32 electrodes, source localization allows to gain valuable insight about the underlying sources, particularly in applications with well-defined focal activity such as epileptic spikes”. Anyway, we are conscious that higher density EEG recordings may benefit our findings. However, we should also add that the results we have presented in this work are those which exhibited significant differences at a level of 0.01 threshold after correcting by multi-comparisons, which is a strong statistical result.

5.2. iCoh as acausal information flow measurement

The isolated effective coherence (iCoh) Pascual-Marqui et al. (2014a, 2014b) is a relatively new technique. It has been shown both in simulations as well as in real data to achieve better performance than the most popular method currently used for EEG effective connectivity, the Partial Directed Coherence (PDC) (Baccala and Sameshima, 2001). It has also been successfully used in different EEG functional connectivity research, as compiled in Section 2.4.4. At the moment of writing this paper, the method has 51 citations in Google Scholar.

However, additional research to assess its validity in more EEG scenarios will increase the understanding of this technology.

5.3. Summarizing the information using the AAL brain segmentation

Another point in this paper which may be controversial is the use of the AAL segmentation to summarize the information by brain regions instead of individual sources. Some AAL regions are large so providing a coarse segmentation of the brain. Calculating the average of many sources in the same region implies the possibility of losing real activations in small areas of the region, which are masked by the average of the whole region. But it is not a real risk of creating spurious correlations. In this sense, we may be losing possible connected areas rather than creating non existing ones. This possibility may be attenuated by using other finer brain segmentation which divides the brain in smaller regions. This issue may affect the correlation analysis, which is only used for obtaining the areas with higher connectivity differences. However, for the causality analysis we do not average the whole region, but we find the sources with the highest correlations within the region and then define a small ROI around them. Nevertheless, this is an aspect that can be improved in our future work.

5.4. Comparisons against a sample of functionally healthy children

Finally, although the results of comparing the functional brain connectivity between dysphonetic dyslexia and non-specific reading delay children are quite interesting, it would be very important to compare these two groups with other subtypes of dyslexia and a group of functionally healthy children. We are in the process of collecting samples of functionally healthy children, as well as samples of children with dyseidetic and mixed dyslexia subtypes to complete our comparisons.

6. Conclusions

In conclusion, we may affirm that this study represents the first attempt to demonstrate which type of EEG connectivity exists in dyslexic subjects using the classification in subtypes proposed by Boder's model. The results show different neurophysiological patterns in DD subjects and in NSRD subjects. This different pattern is also clinically confirmed by applying the direct reading and writing test. These results need further confirmation by applying this method to other dyslexia subtypes such as dyseidetic and mixed (dysphonetic + dyseidetic). The fact that these differences were found in a resting EEG should not be underestimated. It could therefore be said that there is a basic neurophysiological condition that distinguishes these two groups. Reading tasks have already highlighted differences in reading related potentials between dysphonetic and normal subjects (Casarotto et al., 2007a, 2007b; Chiarenza et al., 2013; Chiarenza, 2017). The use of these new methodologies during activation tasks could further confirm the existence of these subtypes and further validate the Boder's model. The brain areas involved in the reading process are certainly much more numerous than those described in this work. However, we assume that the description of dynamic connectivity processes even in a resting EEG in dyslexic subjects can be immediately useful not only for research but also for clinical purposes, like evaluating how different rehabilitation strategies, i.e. speech therapy and neurofeedback, impact on the brain connectivity in these groups of subjects.

Appendix A. Supplementary data

Supplementary data to this article can be found online at <https://doi.org/10.1016/j.ijpsycho.2020.04.021>.

References

- Abercrombie, M.L.J., Lindon, R.L., Tyson, M.C., 1964. Associated movements in normal and physically handicapped children. *Dev. Med. Child Neurol.* 6, 573–680. <https://doi.org/10.1111/j.1469-8749.1964.tb02795.x>.
- Adams, R.M., Kocsis, J.J., Estes, R.E., 1974. Soft neurological signs in learning disabled children and controls. *Am. J. Dis. Child.* 128 (5), 614–618. <https://doi.org/10.1001/archpedi.1974.02110300024004>.
- Akaike, H., 1968. On the use of a linear model for the identification of feedback systems. *Ann. Inst. Stat. Math.* 20 (1), 425–439. <https://doi.org/10.1007/BF02911655>.
- Arns, M., Peters, S., Breteler, R., Verhoeven, L., 2007. Different brain activation patterns in dyslexic children: evidence from EEG power and coherence patterns for the double-deficit theory of dyslexia. *J. Integr. Neurosci.* 6 (1), 175–190. <https://doi.org/10.1142/S0219635207001404>.
- Asadzadeh, S., Rezaii, T.Y., Beheshti, S., Delpak, A., Meshgini, S., 2019. A Systematic Review of EEG Source Localization Techniques and Their Applications on Diagnosis of Brain Abnormalities.
- Babiloni, C., Binetti, G., Cassetta, E., Carboneschi, D., Dal Forno, G., Del Percio, C., Rossini, P.M., 2004. Mapping distributed sources of cortical rhythms in mild Alzheimer's disease. A multicentric EEG study. *NeuroImage* 22 (1), 57–67. <https://doi.org/10.1016/j.neuroimage.2003.09.028>.
- Baccala, L.A., Sameshima, K., 2001. Partial directed coherence: a new concept in neural structure determination. *Biol. Cybern.* 84, 463–474.
- Baccala, L.A., Sameshima, K., Takahashi, D.Y., 2007. Generalized partial directed coherence. *Digital Signal Process.* 3, 163–166.
- Bakker, D.J., 1992. Neuropsychological classification and treatment of dyslexia. *J. Learn. Disabil.* 25, 102–109. <https://doi.org/10.1177/002221949202500203>.
- Becker, J., Velasco, M., Harmony, T., Marosi, E., Landázuri, A.M., 1987. Electroencephalographic characteristics of children with learning disabilities. *Clin. Electroencephalogr.* 18, 93–101.
- Biancardi, A., Morioni, E., Pieretti, E., 2004. BDE, Batteria per la discalculia evolutiva. Omega, Torino, Italy.
- Biscay, R.J., Bosch-Bayard, J.F., Pascual-Marqui, R.D., 2018. Unmixing EEG inverse solutions based on brain segmentation. *Front. Neurosci.* 12 (MAY). <https://doi.org/10.3389/fnins.2018.00325>.
- Boder, E., 1973. Developmental dyslexia: a diagnostic approach based on three typical reading-spelling patterns. *Dev. Med. Child Neurol.* 15 (5), 663–687. <https://doi.org/10.1111/j.1469-8749.1973.tb05180.x>.
- Bookheimer, S.Y., Zeffiro, T.A., Blaxton, T., Gaillard, W., Theodore, W., 1995. Regional cerebral blood flow during object naming and word reading. *Hum. Brain Mapp.* 3, 93–106.
- Bosch-Bayard, J., Peluso, V., Galan, L., Valdes Sosa, P., Chiarenza, G.A., 2018. Clinical and electrophysiological differences between subjects with dysphonetic dyslexia and non-specific reading delay. *Brain Sci* 8 (9), 172–200. <https://doi.org/10.3390/brainsci8090172>.
- Brauchli, C., Elmer, S., Rogenmoser, L., Burkhard, A., Jäncke, L., 2018. Top-down signal transmission and global hyperconnectivity in auditory-visual synesthesia: evidence from a functional EEG resting-state study. *Hum. Brain Mapp.* 39 (1), 522–531. <https://doi.org/10.1002/hbm.23861>.
- Bruininks, V.L., Bruininks, R.H., 1977. Motor proficiency of learning disabled and non-disabled students. *Percept. Mot. Skills* 44, 1131–1137. <https://doi.org/10.2466/pms.1977.44.3c.1131>.
- Byring, R.F., Jarvilehto, T., 1985. Auditory and visual evoked potentials of schoolboys with spelling disabilities. *Dev. Med. Child Neurol.* 27, 141–148.
- Byring, R.F., Salmi, T., Sainio, K., Orn, H., 1991. EEG in children with spelling disabilities. *Electroencephalogr. Clin. Neurophysiol.* 79, 247–255. [https://doi.org/10.1016/0013-4694\(91\)90119-0](https://doi.org/10.1016/0013-4694(91)90119-0).
- Cao, Z., Lin, C.T., Chuang, C.H., Lai, K.L., Yang, A.C., Fuh, J.L., Wang, S.J., 2016. Resting-state EEG power and coherence vary between migraine phases. *J. Headache Pain* 17 (1), 1–9. <https://doi.org/10.1186/s10194-016-0697-7>.
- Casarotto, S., Ricciardi, E., Sani, L., Guazzelli, M., Pietrini, P., Chiarenza, G.A., 2007a. ERPs disclose the specificity of spatio-temporal patterns of brain activity during self-paced reading aloud. *NeuroImage* 36 (Suppl. 1), 169 (T-AM).
- Casarotto, S., Ricciardi, E., Sani, L., Guazzelli, M., Pietrini, P., Chiarenza, G.A., 2007b. Single-letter reading elicits a different spatio-temporal modulation of brain activity in dyslexic children as compared to healthy controls. *NeuroImage* 36 (1), 171 (T-PM). [13th Annual Meeting of the Organization for Human Brain Mapping, 9-15 June 2007, Chicago (IL) - USA, poster].
- Chabot, R.J., di Michele, F., Pritchep, L., John, E.R., 2001. The clinical role of computerized EEG in the evaluation and treatment of learning and attention disorders in children and adolescents. *J. Neuropsychiatry Clin. Neurosci.* 13 (2), 171–186. <https://doi.org/10.1176/jnp.13.2.171>.
- Chiarenza, G.A., 1990. Motor-perceptual function in children with developmental reading disorders: neuropsychophysiological analysis. *J. Learn. Disabil.* 23, 375–385. <https://doi.org/10.1177/002221949002300609>.
- Chiarenza, G.A., 2010. Test diretto di lettura e scrittura, DTLS, 2nd edn. Centro Internazionale Disturbi di Apprendimento, Attenzione, Iperattività (CIDAADI), Milan.
- Chiarenza, G.A., 2017. Normal and abnormal reading processes in children. *Neuropsychophysiological studies*. In: Collura, Thomas F., Frederick, Jon A. (Eds.), *Handbook of Clinical QEEG and Neurotherapy*. Routledge, 711 Third Avenue, New York, pp. 235–249.
- Chiarenza, G.A., Bindelli, D., 2001. Il test diretto di lettura e scrittura (DTLS): Versione computerizzata e dati normativi. *Giornale Neuropsichiatria dell'Età Evolutiva* 21, 163–179.
- Chiarenza, G.A., Papakostopoulos, D., Guareschi Cazzullo, A., Giordana, F., Giammari

- Aldè, G., 1982. Movement related brain macro potentials during skilled performance task in children with learning disabilities. In: Chiarenza, G.A., Papakostopoulos, D. (Eds.), *Clinical Application of Cerebral Evoked Potentials in Pediatric Medicine*. 1982. Excerpta Medica, Amsterdam, pp. 259–292.
- Chiarenza, G.A., Olgiati, P., Trevisan, C., De Marchi, I., Casarotto, S., 2013. Reading aloud: a psychophysiological investigation in children. *Neuropsychologia* 51 (3), 425–436. <https://doi.org/10.1016/j.neuropsychologia.2012.11.030>.
- Cohen, L., Dehaene, S., 2004. Specialization within the ventral stream: the case for the visual word form area. *NeuroImage* 22 (1), 466–476. <https://doi.org/10.1016/j.neuroimage.2003.12.049>.
- Cohen, L., Dehaene, S., Naccache, L., Lehéricy, S., Dehaene-Lambertz, G., Hénaff, M.-A., Michel, F., 2000. The visual word form area. Spatial and temporal characterization of an initial stage of reading in normal subjects and posterior split-brain patients. *Brain* 123 (2), 291–307. <https://doi.org/10.1016/10.1093/brain/123.2.291>.
- Connolly, K., Stratton, P., 1968. Developmental changes in associated movements. *Dev. Med. Child Neurol.* 10, 49–56. <https://doi.org/10.1111/j.1469-8749.1968.tb02837.x>.
- Corbetta, M., Miezin, F.M., Dobmeyer, S., Shulman, G.L., Petersen, S.E., 1991. Selective and divided attention during visual discriminations of shape, color, and speed: functional anatomy by positron emission tomography. *J. Neurosci.* 11, 2383–2402.
- Cornoldi, C., Cazzola, C., 2003. AC-MT 11–14: Test di valutazione delle abilità di calcolo e problem solving dagli 11 ai 14 Anni. Erickson, Trento, Italy.
- Cornoldi, C., Colpo, G., 2011. Prove di lettura MT-2 per la scuola primaria. *Organizzazioni Speciali*, Firenze, Italy.
- Cornoldi, C., Colpo, G., 2012. Nuove prove di lettura MT per la scuola secondaria di I grado. *Organizzazioni Speciali*, Firenze, Italy.
- Cornoldi, C., Lucangeli, D., Bellina, M., 2002. Test AC-MT 6–11: Test di valutazione delle abilità di calcolo. Erickson, Trento, Italy.
- De Sonneville, L.M., 2014. *Handbook Amsterdam Neuropsychological Tasks*. Boom Test Publisher, Amsterdam, The Netherlands.
- Dehaene, S., Cohen, L., Sigman, M., Vinckier, F., 2005. The neural code for written words: a proposal. *Trends Cogn. Sci.* 9 (7), 335–341. <https://doi.org/10.1016/j.tics.2005.05.004>.
- Denckla, H.B., 1973. Development of speed in repetitive and successive finger-movements in normal children. *Dev. Med. Child Neurol.* 15 (5), 635–645. <https://doi.org/10.1111/j.1469-8749.1973.tb05174.x>.
- Denhoff, E., Siqueland, M., Konich, M., Hainsworth, P., 1968. Developmental and predictive characteristics of items from the meeting school screening test. *Dev. Med. Child Neurol.* 10 (2), 220–232. <https://doi.org/10.1111/j.1469-8749.1968.tb02871.x>.
- Di Brina, C., Rossini, G., 2011. BHK Scala sintetica per la valutazione della scrittura in età evolutiva. Erickson, Trento, Italy.
- Diagnostic and Statistical Manual of Mental Disorders, 5th ed. American Psychiatric Association, Arlington, VA, USA.
- Diamagnet, J.F., Price, C., Wise, R., Frackowiak, R.S.J., 1994a. A PET study of cognitive strategies in normal subjects during language tasks. Influence of phonetic ambiguity and sequence processing on phoneme monitoring. *Brain* 117, 671–682.
- Diamagnet, J.F., Price, C., Wise, R., Frackowiak, R.S.J., 1994b. Differential activation of right and left posterior sylvian regions by semantic and human subjects. *Neurosci. Lett.* 182, 25–28.
- Duffy, F.H., Denckla, M.B., Bartels, P.H., Sandini, G., 1980. Dyslexia: regional differences in brain electrical activity by topographic mapping. *Ann. Neurol.* 7 (5), 412–420. <https://doi.org/10.1002/ana.410070505>.
- Eugene, A.R., Masiak, J., Kapica, J., Masiak, M., Weinshilboun, R.M., 2015. Electrophysiological neuroimaging using sLORETA comparing 22 age matched male and female schizophrenia patients. *Hospital Chronicles = Nosokomeiaka Chronika* 10 (2), 91–98. <https://doi.org/10.2015/hc.v10i2.696>.
- Evans, A.C., Collins, D.L., Mills, S.R., Brown, E.D., Kelly, R.L., Peters, T.M., 1993. 3D statistical neuroanatomical models from 305 MRI volumes. In: *Proceedings of the IEEE - Nuclear Science Symposium and Medical Imaging Conference*, San Francisco, CA, USA, pp. 1813–1817.
- Evans, A.C., Collins, D.L., Neelin, P., MacDonald, D., Kamber, M., Marrett, T.S., 1994. In: *Thatcher, R., Hallett, M. (Eds.), Three-dimensional Correlative Imaging: Applications in Human Brain Mapping*.
- Fan, Q., Davis, N., Anderson, A.W., Cutting, L.E., 2014. Thalamo-cortical connectivity: what can diffusion tractography tell us about reading difficulties in children? *Brain Connect.* 4 (6), 428–439. <https://doi.org/10.1089/brain.2013.0203>.
- Feng, I., Li, L., Zhang, M., Yang, X., Tian, M., Xie, Lu, W.Y., Liu, L., Bélanger, N.N., Meng, X., 2017. Dyslexic children show atypical cerebellar activation and cerebro-cerebellar functional connectivity in orthographic and phonological processing. *Cerebellum* 16 (2), 496–507. <https://doi.org/10.1007/s12311-016-0829-2>.
- Fernandez Guerrero, A., Achermann, P., 2018. Intracortical causal information flow of oscillatory activity (effective connectivity) at the sleep onset transition. *Front. Neurosci.* 12, 912. <https://doi.org/10.3389/fnins.2018.00912>.
- Finn, E.S., Papademetris, X., Shaywitz, S.E., Shaywitz, B.A., Constable, R.T., 2017. Disruption of functional networks in dyslexia: a whole-brain, data-driven analysis of connectivity. *Biol. Psychiatry* 76 (5), 397–404. <https://doi.org/10.1016/j.biopsych.2013.08.031>.
- Flowers, D.L., Wood, F.B., Naylor, C.E., 1991. Regional cerebral blood flow correlates of language processes in reading disabilities. *Arch. Neurol.* 48, 637–643.
- Fog, E., Fog, M., 1963. Cerebral inhibition examined by associated movements. In: *Satz, P., Ross, J.J. (Eds.), Minimal Cerebral Dysfunction. Clinics in Developmental Medicine*, N. 10. Spastics Society with Heinemann Medical, London.
- Frye, R.E., Liederman, J., McGraw Fisher, J., Wu, M.H., 2012. Laterality of temporoparietal causal connectivity during the pre-stimulus period correlates with phonological decoding task performance in dyslexic and typical readers. *Cereb. Cortex* 22 (8), 1923–1934. <https://doi.org/10.1093/cercor/bhr265>.
- Galan, L., Biscay, R., Valdes, P., Neira, L., Virues, T., 1994. Multivariate statistical brain electromagnetic mapping. *Brain Topogr.* 7 (1), 17–28. <https://doi.org/10.1007/BF01184834>.
- Gazzaniga, M.S., Ivry, R.B., Mangun, G.R., 2009. *Cognitive Neuroscience, the Biology of the Mind*, third edition. W.W. Norton, publishers, pp. 395–401.
- Granger, C.W.J., 1969. Investigating causal relations by econometric models and cross-spectral methods. *Econometrica* 37 (3), 424–438.
- Grech, R., Cassar, T., Muscat, J., Camilleri, K.P., Fabri, S.G., Zervakis, M., ... Vanrumste, B., 2008. Review on solving the inverse problem in EEG source analysis. *Imaging* 33, 1–33. <https://doi.org/10.1186/1743-0003-5-25>.
- Harmony, T., 1988. Psychophysiological evaluation of children's neuropsychological disorders. In: *Reynolds, C.R. (Ed.), Handbook of Child Clinical Neuropsychology*. Plenum, New York, pp. 265–290.
- Harmony, T., Hinojosa, G., Marosi, E., Becker, J., Rodriguez, M., Reyes, A., Rocha, C., 1990. Correlation between EEG spectral parameters and an educational evaluation. *Int. J. Neurosci.* 54, 147–155.
- Horowitz-Kraus, T., Holland, S.K., 2015. Greater functional connectivity between reading and error-detection regions following training with the reading acceleration program in children with reading difficulties. *Ann. Dyslexia* 65 (1), 1–23. <https://doi.org/10.1007/s11881-015-0096-9>.
- Horowitz-Kraus, T., Buck, C., Dormann, D., 2016. Altered neural circuits accompany lower performance during narrative comprehension in children with reading difficulties: an fMRI study. *Ann. Dyslexia* 66 (3), 301–318. <https://doi.org/10.1007/s11881-016-0124-4>.
- Hughes, J.R., 1978. Electroencephalographic and neurophysiological studies in dyslexia. In: *Benton, A., Peal, D. (Eds.), Dyslexia: An Appraisal of Current Knowledge*. Oxford University Press, New York, pp. 207–240.
- Imperatori, C., Farina, B., Quintiliani, M.I., Onofri, A., Castelli Gattinara, P., Lepore, M., ... Della Marca, G., 2014. Aberrant EEG functional connectivity and EEG power spectra in resting state post-traumatic stress disorder: A sLORETA study. *Biol. Psychol.* 102 (1), 10–17. <https://doi.org/10.1016/j.biopsycho.2014.07.011>.
- Jansen, B.H., 1979. Usefulness of autoregressive models to classify EEG-segments. *Biomed. Tech.* 24 (9), 216–223. <https://doi.org/10.1515/bmte.1979.24.9.216>.
- John, E.R., 1981. Neurometric evaluation of brain function related to learning disorders. *Acta Neurol. Scand.* 64 (89), 87–100. <https://doi.org/10.1111/j.1600-0404.1981.tb02367.x>.
- John, E.R., Prichep, L.S., Ahn, H., Easton, P., Fridman, J., Kaye, H., 1983. Neurometric evaluation of cognitive dysfunctions and neurological disorders in children. *Prog. Neurobiol.* 21 (4), 239–290. [https://doi.org/10.1016/0301-0082\(83\)90014-X](https://doi.org/10.1016/0301-0082(83)90014-X).
- Kamiński, M.J., Blinowska, K.J., 1991. A new method of the description of the information flow in the brain structures. *Biol. Cybern.* 65 (3), 203–210. <https://doi.org/10.1007/BF00198091>.
- Kennard, M.A., 1960. Value of equivocal signs in neurological diagnosis. *Neurology*, Minneap 10 (8), 753–764. <https://doi.org/10.1212/WNL.10.8.753>.
- Kiyosawa, M., Inaue, C., Kawasaki, T., Tokoro, T., Ishii, K., Ohyawa, M., Senda, M., Sama, Y., 1996. Functional neuroanatomy of visual object naming: a PET study. *Graefes Archive for Clinical & Experimental Ophthalmology* 234 (2), 110–115.
- Klicpera, C., Wolff, P.H., Drake, C., 1981. Bimanual co-ordination in adolescent boys with reading retardation. *Develop. Med. Child Neurol.* 23 (5), 617–625. <https://doi.org/10.1111/j.1469-8749.1981.tb02043.x>.
- Koyama, M.S., Di Martino, A., Zuo, X.N., Kelly, C., Mennes, M., Jugtar, D.R., Castellanos, F.X., Milham, M.P., 2011. Resting-state functional connectivity indexes reading competence in children and adults. *J. Neurosci.* 31 (23), 8617–8624. <https://doi.org/10.1523/JNEUROSCI.4865-10.2011>.
- Kronbichler, M., Hutzler, F., Staffen, W., Mair, A., 2006. Evidence for a dysfunction of left posterior reading areas in German dyslexic readers. *Neuropsychologia* 44 (10), 1822–1832. <https://doi.org/10.1016/j.neuropsychologia.2006.03.010>.
- Lewis, F.D., Bell, D.B., Anderson, R.P., 1970. Relationship of motor proficiency and reading retardation. *Percept. Motor Skills* 31, 395–401. <https://doi.org/10.2466/pms.1970.31.2.395>.
- Llinás, R., 1993. Is dyslexia a dyschronia? *Ann. N. Y. Acad. Sci.* 682, 48–56. <https://doi.org/10.1111/j.1749-6632.1993.tb22958.x>.
- Lou, C., Duan, X., Altarelli, I., Sweeney, J.A., Ramus, F., Zhao, J., 2019. White matter network connectivity deficits in developmental dyslexia. *Hum. Brain Mapp.* 40 (2), 505–516. <https://doi.org/10.1002/hbm.24390>.
- Lueck, C.J., Zeki, S., Friston, K.J., Deiber, M.-P., Cope, P., Cunningham, V.J., Lammertsma, A.A., Kennard, C., Frackowiak, R.S.J., 1989. The colour centre in the cerebral cortex of man. *Nature* 340, 386–389.
- Mechelli, A., Friston, K.J., Price, K.J., 2000. The effects of presentation rate during word and pseudoword reading: a comparison of PET and fMRI. *J. Cogn. Neurosci.* 12 (2), 145–156. <https://doi.org/10.1162/089992900564000>.
- Michael, D., Houchin, J., 1979. Automatic EEG analysis: a segmentation procedure based on the autocorrelation function. *Electroencephalogr. Clin. Neurophysiol.* 46 (2), 232–235. [https://doi.org/10.1016/0013-4694\(79\)90075-0](https://doi.org/10.1016/0013-4694(79)90075-0).
- Michel, C.M., Brunet, D., 2019. EEG source imaging: a practical review of the analysis steps. *Front. Neurol.* 10 (APR). <https://doi.org/10.3389/fneur.2019.00325>.
- Morken, F., Hellanda, T., Hugdahl, K., Specht, K., 2017. Reading in dyslexia across literacy development: a longitudinal study of effective connectivity. *NeuroImage* 144 (Part A), 92–100. <https://doi.org/10.1016/j.neuroimage.2016.09.060>.
- Muller-Axt, C., Anwander, A., von Kriegstein, K., 2017. Altered structural connectivity of the left visual thalamus in developmental dyslexia. *Curr. Biol.* 27 (4), 3692–3698. <https://doi.org/10.1016/j.cub.2017.10.034>. (23).
- Nakamichi, N., Takamoto, K., Nishimaru, H., Fujiwara, K., Takamura, Y., Matsumoto, J., Noguchi, M., Nishijo, H., 2018. Cerebral hemodynamics in speech-related cortical areas: articulation learning involves the inferior frontal gyrus, ventral sensory-motor

- cortex, and parietal temporal sylvian area. *Front. Neurol.* 9. <https://doi.org/10.3389/fneur.2018.00939>.
- Nicolson, R.I., Fawcett, A.J., 2005. Developmental dyslexia, learning and the cerebellum. *J. Neural Transm.* 69, 19–36. <https://doi.org/10.1007/s11111-005-0001-0>.
- Niedermeyer, E., Schomer, D.L., Lopes da Silva, F.H., 2010. *Niedermeyer's Electroencephalography: Basic Principles, Clinical Applications, and Related Fields*. Wolters Kluwer Health.
- Nunez, P.L., Srinivasan, R., 2009. *Electric Fields of the Brain: The Neurophysics of EEG*. Electric Fields of the Brain: The Neurophysics of EEG. <https://doi.org/10.1093/acprof:oso/9780195050387.001.0001>.
- Owen, F.W., Adams, P.A., Forrest, T., Soltz, L.M., Fisher, S., 1971. Learning disorders in children. *Monogr. Soc. Child Develop. Serial(144)*.
- Pascual-Marqui, R.D., 2002. Standardized low-resolution brain electromagnetic tomography (sLORETA): technical details. *Methods Find. Exp. Clin. Pharmacol.* 24 (D), 5–12.
- Pascual-Marqui, R.D., Biscay, R.J., Bosch-Bayard, J., Lehmann, D., Kochi, K., Kinoshita, T., Sadato, N., 2014a. Assessing direct paths of intracortical causal information flow of oscillatory activity with the isolated effective coherence (iCoh). *Front. Hum. Neurosci.* 8 (June), 1–12. <https://doi.org/10.3389/fnhum.2014.00448>.
- Pascual-Marqui, R.D., Biscay, R., Bosch-Bayard, J., Lehmann, D., Kochi, K., Yamada, N., ... Sadato, N., 2014b. Isolated effective coherence (iCoh): causal information flow excluding indirect paths. Retrieved from. <http://arxiv.org/abs/1402.4887>.
- Penolazzi, B., Spironelli, C., Vio, C., Angrilli, A., 2010. Brain plasticity in developmental dyslexia after phonological treatment: a beta EEG band study. *Behav. Brain Res.* 209 (1), 179–182. <https://doi.org/10.1016/j.bbr.2010.01.029>.
- Praetorius, H.M., Bodenstein, G., Creutzfeldt, O.D., 1977. Adaptive segmentation of EEG records: a new approach to automatic EEG analysis. *Electroencephalogr. Clin. Neurophysiol.* 42 (1), 84–94. [https://doi.org/10.1016/0013-4694\(77\)90153-5](https://doi.org/10.1016/0013-4694(77)90153-5).
- Price, C.J., Devlin, J.T., 2011. The interactive account of ventral occipito-temporal contributions to reading. *Trends Cogn. Sci.* 15 (6), 246–253. <https://doi.org/10.1016/j.tics.2011.04.001>.
- Price, C.J., Mechelli, A., 2005. Reading and reading disturbance. *Curr. Opin. Neurobiol.* 15, 231–238. <https://doi.org/10.1016/j.conb.2005.03.003>.
- Price, C.J., Wise, R.J., Watson, J.D., Patterson, K., Howard, D., Frackowiak, R.S., 1994. Brain activity during reading: the effects of exposure duration and task. *Brain* 117, 1255–1269.
- Pugh, K.R., Mencl, W.E., Jenner, A.R., Katz, L., Frost, S.J., Lee, J.R., Shaywitz, S.E., Shaywitz, B.A., 2000. Functional neuroimaging studies of reading and reading disability (developmental dyslexia). *Ment. Retard. Dev. Disabil. Res. Rev.* 6, 207–213. [https://doi.org/10.1002/1098-2779\(2000\)6:3<207::AID-MRDD8>3.0.CO;2-P](https://doi.org/10.1002/1098-2779(2000)6:3<207::AID-MRDD8>3.0.CO;2-P).
- Pyfer, H.L., Carlson, B.R., 1972. Characteristic motor development of children with learning disabilities. *Percept. Mot. Skills* 35, 291–296. <https://doi.org/10.2466/pms.1972.35.1.291>.
- Richlan, F., 2012. Developmental dyslexia: dysfunction of a left hemisphere reading network. *Front. Hum. Neurosci.* 6, 1–5. <https://doi.org/10.3389/fnhum.2012.00120>.
- Richlan, F., Kronbichler, M., Wimmer, H., 2011. Meta-analyzing brain dysfunctions in dyslexic children and adults. *NeuroImage* 56, 1735–1742. <https://doi.org/10.1016/j.neuroimage.2011.02.040>.
- Riera, J.J., Fuentes, M.E., 1998. Electric lead field for a piecewise homogeneous volume conductor model of the head. *IEEE Trans. Biomed. Eng.* 45 (6), 746–753. <https://doi.org/10.1109/10.678609>.
- Rumsey, J.M., Andreasen, P., Zametkin, A.J., Aquino, T., King, A.C., Hamburger, S.D., Anita Pikus, A., Rapoport, J.L., Cohen, R.M., 1992. Failure to activate the left temporoparietal cortex in dyslexia: an oxygen 15 positron emission tomographic study. *Arch. Neurol.* 49 (5), 527–534. <https://doi.org/10.1001/archneur.1992.00530290115020>.
- Ryynänen, O.R.M., Hyttinen, J.A.K., Laarne, P.H., Malmivuo, J.A., 2004. Effect of electrode density and measurement noise on the spatial resolution of cortical potential distribution. *IEEE Trans. Biomed. Eng.* 51 (9), 1547–1554. <https://doi.org/10.1109/TBME.2004.828036>.
- Saito, Y., Harashima, H., 1981. Tracking of information within multichannel EEG record-causal analysis in EEG. In: Yamaguchi, N., Fujisawa, K. (Eds.), *Recent Advances in EEG and EMG Data Processing*. Elsevier, North-Holland, Amsterdam, pp. 133–146.
- Sartori, G., Job, R., Tressoldi, P.E., 2007. *Batteria per la valutazione della dislessia e disortografia evolutiva. DDE-2. Organizzazioni Speciali*, Firenze, Italy.
- Schurz, M., Wimmer, H., Richlan, F., Ludersdorfer, P., Klackl, J., Kronbichler, M., 2015. Resting-state and task-based functional brain connectivity in developmental dyslexia. *Cereb. Cortex* 25 (10), 3502–3514. <https://doi.org/10.1093/cercor/bhu184>.
- Shaywitz, B.A., Shaywitz, S.E., Pugh, K.R., Mencl, W.E., Fulbright, R.K., Skudlarski, P., Constable, R.T., Marchione, K.E., Fletcher, J.M., Lyong, G.R., Gore, J.C., 2002. Disruption of posterior brain systems for reading in children with developmental dyslexia. *Biol. Psychiatry* 52, 101–110. [https://doi.org/10.1016/S0006-3223\(02\)01365-3](https://doi.org/10.1016/S0006-3223(02)01365-3).
- Shaywitz, S.E., Shaywitz, B.A., 2005. Dyslexia (specific reading disability). *Biol. Psychiatry* 57, 1301–1309. <https://doi.org/10.1016/j.biopsych.2005.01.043>.
- Song, J., Davey, C., Poulsen, C., Luu, P., Turovets, S., Anderson, E., ... Tucker, D., 2015. EEG source localization: Sensor density and head surface coverage. *J. Neurosci. Methods* 256, 9–21. <https://doi.org/10.1016/j.jneumeth.2015.08.015>.
- Steinmann, S., Amselberg, R., Cheng, B., et al., 2018. The role of functional and structural interhemispheric auditory connectivity for language lateralization. A combined EEG and DTI study. *Sci. Rep.* 8, 15428. <https://doi.org/10.1038/s41598-018-33586-6>.
- Stine, O.C., Saratsiotis, J.M., Mosser, R.S., 1975. Relationships between neurological findings and classroom behavior. *Am. J. Dis. Child.* 129, 1036–1040. <https://doi.org/10.1001/archpedi.1975.02120460024006>.
- Stokić, M., Milosavljević, Z., Subotic, M., 2011. Specific features of brain connectivity during silent reading in children with developmental dyslexia. *Specijalna edukacija i rehabilitacija* 10 (3), 479–492.
- Tressoldi, P., Cornoldi, C., Re, A.M., 2012. *BVSCO-2: Batteria per la valutazione della scrittura e della competenza ortografica-2*. Giunti OS, Firenze, Italy.
- Tzourio-Mazoyer, N., Landeau, B., Papathanassiou, D., Crivello, F., Etard, O., Delcroix, N., Joliot, M., 2002. Automated anatomical labeling of activations in SPM using a macroscopic anatomical parcellation of the MNI MRI single-subject brain. *NeuroImage* 15 (1), 273–289. <https://doi.org/10.1006/nimg.2001.0978>.
- Van der Mark, S., Klaver, P., Kerstin Buchera, K., Maurer, U., Schulz, E., Brem, S., Martin, E., Brandeis, D., 2011. The left occipito-temporal system in reading: disruption of focal fMRI connectivity to left inferior frontal and inferior parietal language areas in children with dyslexia. *NeuroImage* 54 (3), 2426–2436. <https://doi.org/10.1016/j.neuroimage.2010.10.002>.
- Vinckier, F., Dehaene, S., Jobert, A., Dubus, J., Sigman, P.M., Cohen, L., 2007. Hierarchical coding of letter strings in the ventral stream: dissecting the inner organization of the visual word-form system. *Neuron* 55 (1), 143–156. <https://doi.org/10.1016/j.neuron.2007.05.031>.
- Wolff, P.H., Hurwitz, J., 1973. Functional implications of the mentally brain damaged syndrome. *Semin. Psychiat.* 5, 105–115.
- Worsley, K.J., Taylor, J.E., Carbonell, F., Chung, M.K., 2009. SurfStat: a Matlab toolbox for the statistical analysis of univariate and multivariate surface and volumetric data using linear mixed effects models and random field theory. *NeuroImage* 47, S102. [https://doi.org/10.1016/S1053-8119\(09\)70882-1](https://doi.org/10.1016/S1053-8119(09)70882-1).
- Xia, M., Wang, J., He, Y., 2013. BrainNet viewer: a network visualization tool for human brain connectomics. *PLoS One* 8, e68910.
- Žarić, G., Correia, J.M., González, G., Tijms, J.F., van der Molen, M.W., Blomerta, L., Bontea, M., 2017. Altered patterns of directed connectivity within the reading network of dyslexic children and their relation to reading dysfluency. *Dev. Cogn. Neurosci.* 23, 1–13. <https://doi.org/10.1016/j.dcn.2016.11.003>.
- Zatorre, R.J., Meyer, E., Gjedde, A., Evans, A.C., 1996. PET studies of phonetic processing of speech: review, replication, and reanalysis. *Cereb. Cortex* 6, 21–30.
- Zeki, S., Watson, J.D., Lueck, C.J., Friston, K.J., Kennard, C., Frackowiak, R.S., 1991. A direct demonstration of functional specialization in human visual cortex. *J. Neurosci.* 11 (3), 641–649. <https://doi.org/10.1523/JNEUROSCI.11-03-00641.1991>.